



## Review

# A review of catalytic issues and process conditions for renewable hydrogen and alkanes by aqueous-phase reforming of oxygenated hydrocarbons over supported metal catalysts

R.R. Davda, J.W. Shabaker, G.W. Huber, R.D. Cortright<sup>1</sup>, J.A. Dumesic\**Department of Chemical and Biological Engineering, University of Wisconsin, 1415 Engineering Drive, Madison, WI 53706, USA*

Received 23 January 2004; received in revised form 26 April 2004; accepted 30 April 2004

Available online 12 October 2004

**Abstract**

We have recently developed a single-step, low-temperature process for the catalytic production of fuels, such as hydrogen and/or alkanes, from renewable biomass-derived oxygenated hydrocarbons. This paper reviews our work in the development of this aqueous-phase reforming (APR) process to produce hydrogen or alkanes in high yields. First, the thermodynamic and kinetic considerations that form the basis of the process are discussed, after which reaction kinetics results for ethylene glycol APR over different metals and supports are presented. These studies indicate Pt-based catalysts are effective for producing hydrogen via APR. Various reaction pathways may occur, depending on the nature of the catalyst, support, feed and process conditions. The effects of these various factors on the selectivity of the process to make hydrogen versus alkanes are discussed, and it is shown how process conditions can be manipulated to control the molecular weight distribution of the product alkane stream. In addition, process improvements that lead to hydrogen containing low concentrations of CO are discussed, and a dual-reactor strategy for processing high concentrations of glucose feeds is demonstrated. Finally, various strategies are assembled in the form of a composite process that can be used to produce renewable alkanes or fuel-cell grade hydrogen with high selectivity from concentrated feedstocks of oxygenated hydrocarbons.

© 2004 Elsevier B.V. All rights reserved.

*Keywords:* Hydrogen production; Fuel cells; Reforming; Renewable energy; Supported metal catalysts; Hydrocarbon fuels; Renewable alkanes**Contents**

1. Introduction . . . . .	172
2. Aqueous-phase reforming . . . . .	173
2.1. Basis for aqueous-phase reforming process . . . . .	173
2.1.1. Thermodynamic considerations . . . . .	173
2.1.2. Kinetic considerations . . . . .	174
2.2. Factors controlling selectivity for aqueous-phase reforming . . . . .	175
2.2.1. Nature of the catalyst . . . . .	175
2.2.2. Reaction conditions . . . . .	176
2.2.3. Reaction pathways . . . . .	177
2.2.4. Nature of the feed . . . . .	178
2.3. Factors favoring production of heavier alkanes . . . . .	179

\* Corresponding author. Tel.: +1 608 2621095; fax: +1 608 2625434.

*E-mail address:* [dumesic@engr.wisc.edu](mailto:dumesic@engr.wisc.edu) (J.A. Dumesic).<sup>1</sup> Present address: Virent Energy Systems, Madison, WI, USA.

2.4. Producing hydrogen containing low levels of CO: ultra-shift . . . . .	180
2.5. Hydrogen from concentrated glucose feeds . . . . .	181
3. Discussion and overview . . . . .	182
4. Conclusions . . . . .	186
Acknowledgements . . . . .	186
References . . . . .	186

## 1. Introduction

Fuel cells have emerged as promising devices for meeting future global energy needs. In particular, fuel cells that consume hydrogen are environmentally clean, quiet, and highly efficient devices for electrical power generation. While hydrogen fuel cells have a low impact on the environment, current methods for producing hydrogen require high-temperature steam reforming of non-renewable hydrocarbon feedstocks [1,2]. The full environmental benefit of generating power from hydrogen fuel cells is achieved when hydrogen is produced from renewable sources such as solar power and biomass. Biomass and biomass wastes are promising sources for the sustainable production of hydrogen in an age of diminishing fossil fuel reserves. However, conversion of biomass to hydrogen remains a challenge, since processes such as enzymatic decomposition of sugars, steam reforming of bio-oils, and gasification suffer from low hydrogen production rates and/or complex processing requirements [3,4].

The production of hydrogen for fuel cells and other industrial applications from renewable biomass-derived resources is a major challenge as global energy generation moves towards a 'hydrogen society'. Conversion of biomass to hydrogen involves an extraction step to produce an aqueous carbohydrate feed stream from biomass, which can then be processed in a reformer to produce H<sub>2</sub> and CO<sub>2</sub>. The CO<sub>2</sub> green-house gas can then be recycled back into the environment where it is consumed to grow more biomass, and the H<sub>2</sub> can be used for various applications (e.g., fed to a fuel cell, used in a hydrogenation process, consumed in an internal combustion engine, etc.). The development of an efficient reforming process is imperative to make the overall process feasible.

In the present review paper, we show that carbohydrates such as sugars (e.g., glucose) and polyols (e.g., methanol, ethylene glycol, glycerol and sorbitol) can be efficiently converted with water in the aqueous phase over appropriate heterogeneous catalysts at temperatures near 500 K to produce primarily H<sub>2</sub> and CO<sub>2</sub>. Our aqueous-phase reforming (APR) process provides a route to generate hydrogen as a value-added chemical from aqueous-phase carbohydrates found in waste-water from biomass processing (e.g., cheese whey, beer brewery waste-water, sugar

processing), from carbohydrates streams extracted from agricultural products such as corn and sugar beets, and from aqueous carbohydrates extracted by steam-aqueous fractionation of lower-valued hemicellulose from biomass [5–7]. The resulting hydrogen can be purified, if necessary, and utilized as:

1. a chemical feedstock for production of ammonia and fertilizers;
2. a chemical reagent for the future hydrogenation of carbohydrates to produce glycols;
3. a hydrogen-rich gas stream that augments the gas stream from biomass gasification units utilized for the production of liquid fuel via the Fischer–Tropsch process;
4. a future renewable fuel source for PEM fuel cells.

Hydrogen production using APR of carbohydrates has several advantages over existing methods of producing hydrogen via the steam reforming of hydrocarbons:

1. APR eliminates the need to vaporize both water and the oxygenated hydrocarbon, which reduces the energy requirements for producing hydrogen.
2. The oxygenated compounds of interest are nonflammable and non-toxic, allowing them to be stored and handled safely.
3. APR occurs at temperatures and pressures where the water-gas shift reaction is favorable, making it possible to generate hydrogen with low amounts of CO in a single chemical reactor.
4. APR is conducted at pressures (typically 15–50 bar) where the hydrogen-rich effluent can be effectively purified using pressure-swing adsorption or membrane technologies, and the carbon dioxide can also be effectively separated for either sequestration or use as a chemical.
5. APR occurs at low temperatures that minimize undesirable decomposition reactions typically encountered when carbohydrates are heated to elevated temperatures.
6. Production of H<sub>2</sub> and CO<sub>2</sub> from carbohydrates may be accomplished in a single-step, low-temperature process, in contrast to the multi-reactor steam reforming system required for producing hydrogen from hydrocarbons.

Important selectivity challenges govern the production of  $H_2$  by APR, because the mixture of  $H_2$  and  $CO_2$  formed in this process is thermodynamically unstable at low temperatures with respect to the formation of methane. Accordingly, the selective formation of  $H_2$  represents a classic problem in heterogeneous catalysis and reaction engineering: the identification of catalysts and the design of reactors to maximize the yields of desired products at the expense of undesired byproducts formed in series and/or parallel reaction pathways. We show how the hydrogen selectivity can be controlled by altering the nature of catalytically active metal and metal-alloy components, and by choice of catalyst support. We also show how the reforming process can be operated at moderately high feed concentrations of oxygenated hydrocarbons (e.g., 10 wt.%), and we indicate how the APR processes can be conducted to achieve low levels of CO in the gaseous effluent (e.g., lower than 100 ppm). We also demonstrate how the APR process can be designed to favor the formation of heavier alkanes (e.g., hexane) from biomass-derived oxygenated compounds (e.g., glucose). This variation of the APR process provides a means to produce clean alkane streams from renewable resources, thereby providing an application for APR in the interim period until hydrogen fuel cells become more economical.

## 2. Aqueous-phase reforming

### 2.1. Basis for aqueous-phase reforming process

#### 2.1.1. Thermodynamic considerations

Reaction conditions for producing hydrogen from hydrocarbons are dictated by the thermodynamics for the steam reforming of the alkanes to form CO and  $H_2$  (reaction (1)) and the water-gas shift reaction to form  $CO_2$  and  $H_2$  from CO (reaction (2)):

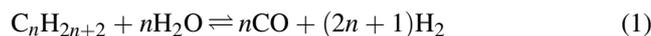


Fig. 1 shows the changes in the standard Gibbs free energy ( $\Delta G^\circ/RT$ ) associated with reaction (1) for a series of alkanes ( $CH_4$ ,  $C_2H_6$ ,  $C_3H_8$ ,  $C_6H_{14}$ ), normalized per mole of CO produced. It can be seen that the steam reforming of alkanes is thermodynamically favorable (i.e., negative values of  $\Delta G^\circ/RT$ ) only at temperatures higher than 675 K (and higher than 900 K for methane reforming). Carbohydrates are oxygenated hydrocarbons having a C:O ratio of 1:1, and these compounds produce CO and  $H_2$  according to reaction (3):



Relevant oxygenated hydrocarbons having a C:O ratio of 1:1 are methanol ( $CH_3OH$ ), ethylene glycol ( $C_2H_4(OH)_2$ ), glycerol ( $C_3H_5(OH)_3$ ), and sorbitol ( $C_6H_8(OH)_6$ ). Importantly, sorbitol is produced via the hydrogenation of glucose

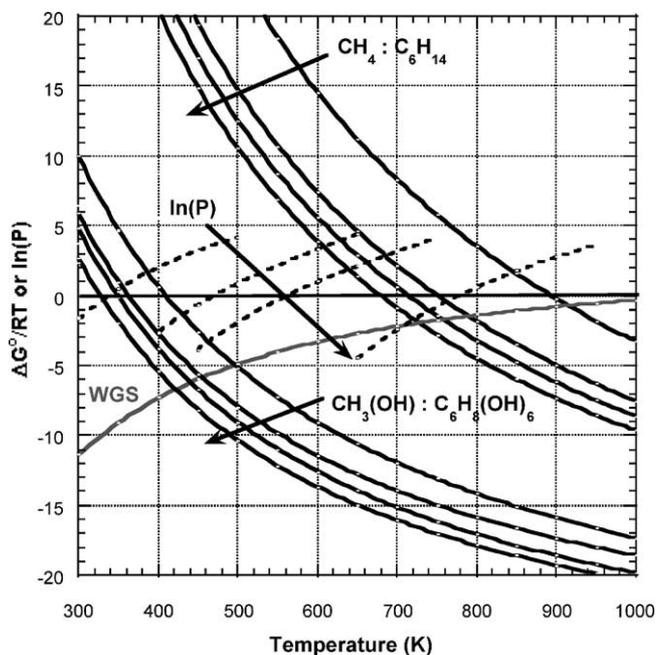


Fig. 1.  $\Delta G^\circ/RT$  vs. temperature for production of CO and  $H_2$  from vapor-phase reforming of  $CH_4$ ,  $C_2H_6$ ,  $C_3H_8$  and  $C_6H_{14}$ ;  $CH_3(OH)$ ,  $C_2H_4(OH)_2$ ,  $C_3H_5(OH)_3$  and  $C_6H_8(OH)_6$ ; and water-gas shift. Dotted lines show values of  $\ln(P)$  for the vapor pressures vs. temperature of  $CH_3(OH)$ ,  $C_2H_4(OH)_2$ ,  $C_3H_5(OH)_3$ , and  $C_6H_8(OH)_6$  (pressure in units of atm).

( $C_6H_8(OH)_6$ ). Fig. 1 shows that steam reforming of these oxygenated hydrocarbons to produce CO and  $H_2$  is thermodynamically favorable at significantly lower temperatures than those required for alkanes with similar number of carbon atoms. Accordingly, the steam reforming of oxygenated hydrocarbons having a C:O ratio of 1:1 would offer a low-temperature route for the formation of CO and  $H_2$ . Fig. 1 also shows that the value of  $\Delta G^\circ/RT$  for water-gas shift of CO to  $CO_2$  and  $H_2$  is more favorable at lower temperatures. Therefore, it might be possible to produce  $H_2$  and  $CO_2$  from steam reforming of oxygenated compounds utilizing a single-step catalytic process, since the water-gas shift reaction is favorable at the same low temperatures at which steam reforming of carbohydrates is possible.

The steam reforming of hydrocarbons typically takes place in the vapor phase. However, vapor-phase steam reforming of oxygenated hydrocarbons at low temperatures may become limited by the vapor pressures of these reactants. Fig. 1 shows the plots of the logarithm of the vapor pressures (in atm) of  $CH_3OH$ ,  $C_2H_4(OH)_2$ ,  $C_3H_5(OH)_3$ , and  $C_6H_8(OH)_6$  versus temperature. It is apparent that the vapor-phase reforming of methanol, ethylene glycol, and glycerol can be carried out at temperatures near 550 K, since the values of  $\Delta G^\circ/RT$  are favorable and the vapor pressures of these oxygenated reactants are higher than 1 atm at this temperature. In contrast, vapor-phase reforming of sorbitol must be carried out at temperatures near 750 K. Importantly, reforming of oxygenated hydrocarbons, if carried out in the liquid phase, would make it possible to produce  $H_2$  from carbohydrate-derived feedstocks (e.g., sorbitol and glucose)

that have limited volatility, thereby taking advantage of single-reactor processing at lower temperatures.

### 2.1.2. Kinetic considerations

Important reaction selectivity issues must be addressed if APR reactions are to be used for the production of  $H_2$  from renewable biomass resources, since the  $H_2$  and  $CO_2$  produced at low temperatures are thermodynamically unstable with respect to alkanes and water. Alkanes (especially  $CH_4$ ) can be formed from the subsequent reaction of  $H_2$  and  $CO/CO_2$  via methanation and Fischer–Tropsch reactions [12–15]. For example, the equilibrium constant at 500 K for the conversion of  $CO_2$  and  $H_2$  to methane ( $CO_2 + 4H_2 \leftrightarrow CH_4 + 2H_2O$ ) is of the order of  $10^{10}$  per mole of  $CO_2$ . Accordingly, selective hydrogen production via APR of oxygenated hydrocarbons would require an efficient catalyst that promotes reforming reactions (C–C scission followed by water-gas shift) and inhibits alkane-formation reactions (C–O scission followed by hydrogenation).

The catalytic activities of different metals for C–C bond breaking during ethane hydrogenolysis have been studied by Sinfelt and Yates [16], and the relative rates for the different metals are shown in Fig. 2. It can be seen that Pt shows reasonable catalytic activity for C–C bond cleavage, although not as high as metals such as Ru, Ni, Ir and Rh. However, an effective catalyst for reforming of ethylene glycol must not only be active for cleavage of the C–C bond, but it must also be active for the water-gas shift reaction to remove CO from the metal surface at the low temperatures of the reforming reaction. In this respect, Grenoble et al. [17] have reported the relative catalytic activities for water-gas shift over different metals supported on alumina, and these data are also shown in Fig. 2. It can be seen that Cu exhibits the highest water-gas

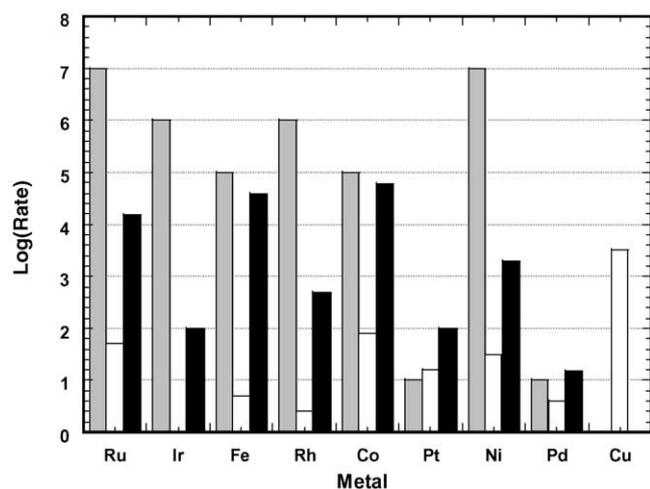


Fig. 2. Relative rates of C–C bond breaking reaction by Sinfelt (grey), water-gas shift reaction by Grenoble, et al. (white), methanation reaction by Vannice (black). The rate of a particular reaction can be compared for the different metals; however, for a specific metal, the absolute rates of the three different reactions cannot be compared relative to each other. Adapted from reference [8].

shift rates among all the metals (although this metal shows no activity for C–C bond breaking), and Pt, Ru and Ni also show appreciable water-gas shift activity. Finally, to obtain a high selectivity for hydrogen production, the catalyst must not facilitate undesired side reactions, such as methanation of CO and Fischer–Tropsch synthesis. Fig. 2 shows the relative rates of methanation catalyzed by different metals supported on silica, as reported by Vannice [15]. It can be seen that Ru, Ni and Rh exhibit the highest rates of methanation, whereas Pt, Ir and Pd show lower catalytic activities for the methanation reaction. Thus, upon comparing the catalytic activities of various metals in Fig. 2, it can be inferred that Pt and Pd should show suitable catalytic activity and selectivity for production of hydrogen by reforming of oxygenated hydrocarbons, which requires reasonably high activity for C–C bond breaking and water-gas shift reactions, and low activity for methanation.

We have recently reported results from periodic density functional theory calculations to probe the nature of surface intermediates that may be formed on Pt(1 1 1) by the decomposition of ethanol [18]. In these calculations, we probed transition states for cleavage of C–C and C–O bonds in these intermediates adsorbed on Pt(1 1 1) to identify and compare the most favorable pathways for cleavage of these bonds in oxygenated hydrocarbons on Pt-based catalysts. We chose ethanol for the study since this molecule is a simple oxygenated hydrocarbon containing a C–C bond.

The strategy for conducting these calculations was first to determine the stabilities of all 24 species (with stoichiometry  $C_2H_xO$ ) that can be formed by removal of hydrogen atoms from ethanol, without cleavage of C–C or C–O bonds. Within each  $C_2H_xO$  isomeric set, the lowest-energy surface species (with respect to gaseous ethanol and clean Pt(1 1 1) slabs) are ethanol, 1-hydroxyethyl ( $CH_3CHOH$ ), 1-hydroxyethylidene ( $CH_3COH$ ), acetyl ( $CH_3CO$ ), ketene ( $CH_2CO$ ), ketylenyl ( $CHCO$ ), and CCO species. The next step in these calculations was to determine the stabilities of all possible reaction products resulting from C–C or C–O bond cleavage (i.e., stabilities of adsorbed O, OH,  $C_2H_x$ , and  $CH_xO$  species). From the results of these calculations it was then possible to determine the energy changes for all possible C–C and C–O cleavage reactions. We then selected those C–C and C–O cleavage reactions with the most favorable energy changes and identified their transition states. In general, the computational time to identify stable adsorbed species is shorter than to identify transition states. Thus, we started with rigorous DFT calculations for transition states corresponding to those reactions with the most favorable energy changes, since these reactions are expected to lead to transition states of low energy. Accordingly, we investigated with rigorous DFT calculations 14 transition states from among the 48 transition states that are possible by cleavage of C–C and C–O bonds in the 24 species that can be formed by dehydrogenation of ethanol. The 1-hydroxyethylidene ( $CH_3COH$ ) species has the lowest-energy transition state for C–O bond cleavage, and the ketylenyl ( $CHCO$ ) species has the lowest-energy transition state for C–C bond cleavage. Based on the results from DFT calculations for

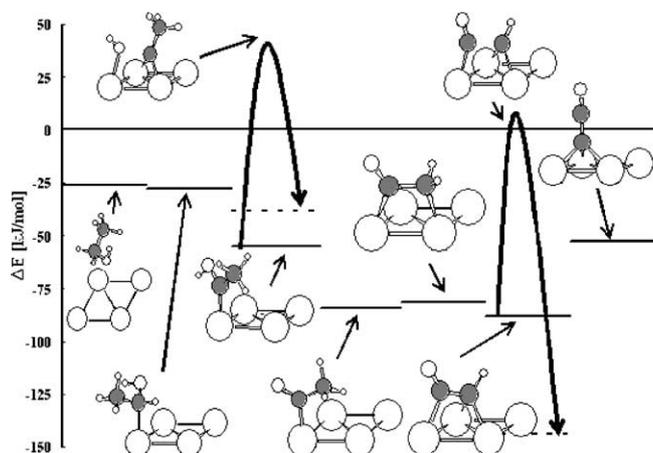


Fig. 3. Reaction energy diagram for ethanol reactions on Pt(111). The reference state is gas phase ethanol and clean slab(s). Removed H atoms and bond cleavage products are each adsorbed on separate slabs. Solid curves represent bond cleavage reactions. Insets show views of stable and transition state species. The large white circles represent Pt atoms, grey medium circles represent C atoms, white medium circles represent O atoms, and the small white circles represent H atoms. Adapted from reference [18].

reactions with favorable energy changes, we generated a linear Brønsted–Evans–Polanyi correlation for the energies of the transition states for C–C and C–O bond cleavage in terms of the energies of the adsorbed products for these reactions. We then used this correlation to estimate the energies of the transition states for the 34 remaining C–C and C–O bond cleavage reactions having less favorable energy changes, from which it was concluded that the energies of these remaining transition states were all significantly higher than the values of the lowest-energy transition energies that we had identified from our rigorous DFT calculations.

Fig. 3 shows a simplified potential energy diagram of the stabilities and reactivities of dehydrogenated species derived from ethanol on Pt(111). Only the most stable species within each isomeric set and the most stable transition states for C–O and C–C bond cleavage are consolidated in this schematic potential energy diagram. Views of adsorbed species and transition states are shown in the insets. It can be seen from Fig. 3 that C–O bond cleavage occurs on more highly hydrogenated species compared to C–C bond cleavage. Importantly, it can be seen that cleavage of the C–C bond in species derived from ethanol should be faster than cleavage of the C–O bond on Pt(111), since the energies with respect to ethanol of the lowest transition states for these reactions are equal to 4 and 42 kJ/mol, respectively. Furthermore, it appears that cleavage of the C–C bond in species derived from ethanol should be faster than cleavage of the C–C bond in ethane on Pt(111). In particular, the electronic energy associated with the formation of this transition state (and adsorbed H-atoms) from ethane is equal to 125 kJ/mol (ref), and this value is significantly higher than the energy of 4 kJ/mol for the transition state controlling C–C cleavage in ethanol.

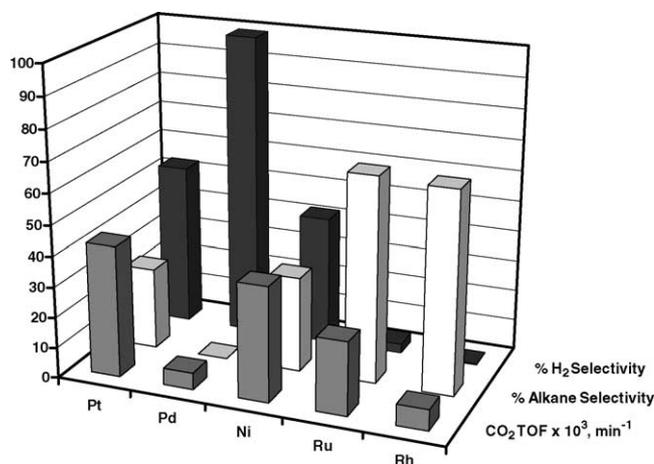


Fig. 4. Comparison of catalytic performance of metals for aqueous-phase reforming of ethylene glycol at 483 K and 22 bar (grey bar: CO<sub>2</sub> TOF × 10<sup>3</sup> (min<sup>-1</sup>); white bar: % alkane selectivity; black bar: % H<sub>2</sub> selectivity). Adapted from reference [8].

## 2.2. Factors controlling selectivity for aqueous-phase reforming

### 2.2.1. Nature of the catalyst

**2.2.1.1. Catalytic metal components.** It is possible to produce hydrogen by steam reforming of methanol over copper-based catalysts at temperatures near 550 K [2,19]. However, copper-based catalysts are not effective for steam reforming of heavier oxygenated hydrocarbons, since these catalysts show low activity for cleavage of C–C bonds [16]. Therefore, it is more likely that effective catalysts for reforming of oxygenated hydrocarbons would be based on Group VIII metals, since these metals generally show higher activities for breaking C–C bonds [16,20]. Aqueous-phase reforming of ethylene glycol over silica-supported Group VIII metal catalysts was conducted in a fixed bed reactor [8,21]. Fig. 4 summarizes the results of these studies at 483 K, and results at 498 K show similar trends. The rate of ethylene glycol reforming (as measured by the rate of CO<sub>2</sub> production) decreases in the following order:

$$\text{Pt} \sim \text{Ni} > \text{Ru} > \text{Rh} \sim \text{Pd} > \text{Ir}$$

The catalysts are also compared based on their selectivity for hydrogen production, which is defined [22] as the number of moles of H<sub>2</sub> in the effluent gas normalized by the number of moles of H<sub>2</sub> that would be present if each mole of carbon in the effluent gas had participated in the ethylene glycol reforming reaction to give 5/2 mol of H<sub>2</sub>. In addition, the alkane selectivity is defined as the moles of carbon in the gaseous alkane products normalized by the total moles of carbon in the gaseous effluent stream. Silica supported Rh, Ru and Ni show low selectivity for production of H<sub>2</sub> and high selectivity for alkane production. Unfortunately, Ni/SiO<sub>2</sub> deactivated under reaction conditions at 498 K.

While Pt, Ni and Ru exhibit relatively high activities for the reforming reaction, only Pt and Pd also show relatively

high selectivity for the production of H<sub>2</sub>. These trends suggest that active catalysts for APR reactions should possess high catalytic activity for the water-gas shift reaction and sufficiently high catalytic activity for cleavage of C–C bonds. Moreover, Pt and Pd catalysts exhibit low activity for the C–O scission reactions and the series methanation and Fischer–Tropsch reactions between the reforming products, CO/CO<sub>2</sub> and H<sub>2</sub>. On this basis, Pt-based catalysts were identified as promising systems for further study. Due to their low cost and good catalytic activity, Ni-based catalysts are also attractive despite their tendency to produce alkanes.

**2.2.1.2. Catalyst supports.** Various supported platinum catalysts were prepared to test the effect of the support on the activity and selectivity for production of hydrogen by aqueous reforming of ethylene glycol [10]. As shown in Fig. 5A, turnover frequencies for production of hydrogen are the highest over Pt-black and Pt supported on TiO<sub>2</sub>, carbon, and Al<sub>2</sub>O<sub>3</sub> (i.e., 8–15 min<sup>-1</sup> at 498 K for 10 wt.% ethylene glycol), while moderate catalytic activity for production of hydrogen is demonstrated by Pt supported on SiO<sub>2</sub>–Al<sub>2</sub>O<sub>3</sub> and ZrO<sub>2</sub> (near 5 min<sup>-1</sup>). Lower turnover frequencies are exhibited by Pt supported on CeO<sub>2</sub>, ZnO, and SiO<sub>2</sub> (less than about 2 min<sup>-1</sup>), which may be due to deactivation caused by hydrothermal degradation of these support materials. As shown in Fig. 5B, catalysts consisting of Pt supported on carbon, TiO<sub>2</sub>, SiO<sub>2</sub>–Al<sub>2</sub>O<sub>3</sub> and Pt-black also lead to the production (about 1–3 min<sup>-1</sup>) of gaseous alkanes and liquid-phase compounds that would lead to alkanes at higher conversions (e.g., ethanol, acetic acid, acetaldehyde). Thus, we conclude that Pt/Al<sub>2</sub>O<sub>3</sub>, and to a lesser extent Pt/ZrO<sub>2</sub> and Pt/TiO<sub>2</sub>, are active as well as selective catalysts for the production of H<sub>2</sub> from liquid-phase reforming of ethylene glycol. By testing a sintered version of our highly dispersed Pt/Al<sub>2</sub>O<sub>3</sub> catalyst (with a dispersion of only 31%), we conclude that effect of support on reforming activity and selectivity is greater than the effect of metal dispersion.

**2.2.1.3. Modified nickel catalysts.** A Sn-promoted Raney-Ni catalyst can be used to achieve good activity, selectivity, and stability for production of hydrogen by APR of biomass-derived oxygenated hydrocarbons [11,23]. This inexpensive material has catalytic properties that are comparable to those of Pt/Al<sub>2</sub>O<sub>3</sub> for production of hydrogen from small oxygenate hydrocarbons, such as ethylene glycol, glycerol, and sorbitol. Rates of hydrogen production by APR of ethylene glycol over Raney-Ni–Sn catalysts with Ni–Sn atomic ratios of up to 14:1 are comparable to 3 wt.% Pt/Al<sub>2</sub>O<sub>3</sub>, based on reactor volume. The addition of Sn to Raney-Ni catalysts significantly decreases the rate of methane formation from series recombination of CO or CO<sub>2</sub> with H<sub>2</sub>, while maintaining high rates of C–C cleavage necessary for production of H<sub>2</sub>. However, it is necessary to operate the reactor near the

bubble-point pressure of the feed and at moderate space-times to achieve high selectivities for production of H<sub>2</sub> over Raney-Ni–Sn catalysts, whereas it is impossible to achieve these high selectivities under any conditions over unpromoted Ni catalysts. These Ni–Sn catalysts illustrate the potential of bimetallic compounds and alloys as new catalysts for the APR process.

### 2.2.2. Reaction conditions

Reaction kinetic measurements were conducted to determine the effects of reaction conditions on the APR of methanol and ethylene glycol over Pt/Al<sub>2</sub>O<sub>3</sub> catalysts [9]. The apparent activation energy barriers for APR of ethylene glycol and methanol (measured under kinetically controlled reaction conditions) at temperatures between 483 and 498 K are equal to 100 and 140 kJ/mol, respectively. At 498 K, these oxygenates have similar reactivity for APR over Pt/Al<sub>2</sub>O<sub>3</sub>, indicating that C–C bond cleavage is not rate limiting for ethylene glycol reforming. Also, both methanol and ethylene glycol reforming are fractional order in feed concentration. The rate of hydrogen production is higher order in methanol (0.8) than ethylene glycol (0.3–0.5), indicating that the surface coverage by species derived from ethylene glycol is higher than from methanol under APR reaction conditions.

Another experimental observation is that the APR reaction is strongly inhibited by system pressure. By assuming that the bubbles inside the reactor consist of water vapor at its vapor pressure, increasing the system pressure at constant temperature increases the partial pressures of the products (i.e., H<sub>2</sub> and CO<sub>2</sub>) according to the following relations:

$$P_{\text{system}} \approx P_{\text{bubble}} = \sum_{\text{feed}} P_i + \sum_{\text{products}} P_j,$$

$$P_j = \frac{P_{j,\text{diluted}}}{\sum_{\text{products}} P_{j,\text{diluted}}} \left( P_{\text{bubble}} - \sum_{\text{feed}} P_i \right)$$

Accordingly, the partial pressure of hydrogen in the reactor can be calculated, and a weak inhibition by hydrogen can thereby be deduced for both feed-stocks (–0.5 order). The inhibiting effect of hydrogen on the rate of reforming could be caused by the blocking of surface sites by adsorbed hydrogen atoms. The increased H<sub>2</sub> and CO<sub>2</sub> partial pressures may also drive the water-gas shift reaction in the reverse direction to increase the CO concentration in the reactor, hence leading to lower rates due to higher coverage of CO on the metal surface. In addition, hydrogen could inhibit the rate by decreasing the surface concentrations of reactive intermediates formed from dehydrogenation of the oxygenated hydrocarbon reactants, as suggested from results of DFT calculations.

The liquid-phase environment of aqueous-phase reforming favors the water-gas shift reaction. Accordingly, low levels of CO (<300 ppm) are detected in the gaseous effluents from APR of methanol and ethylene glycol over

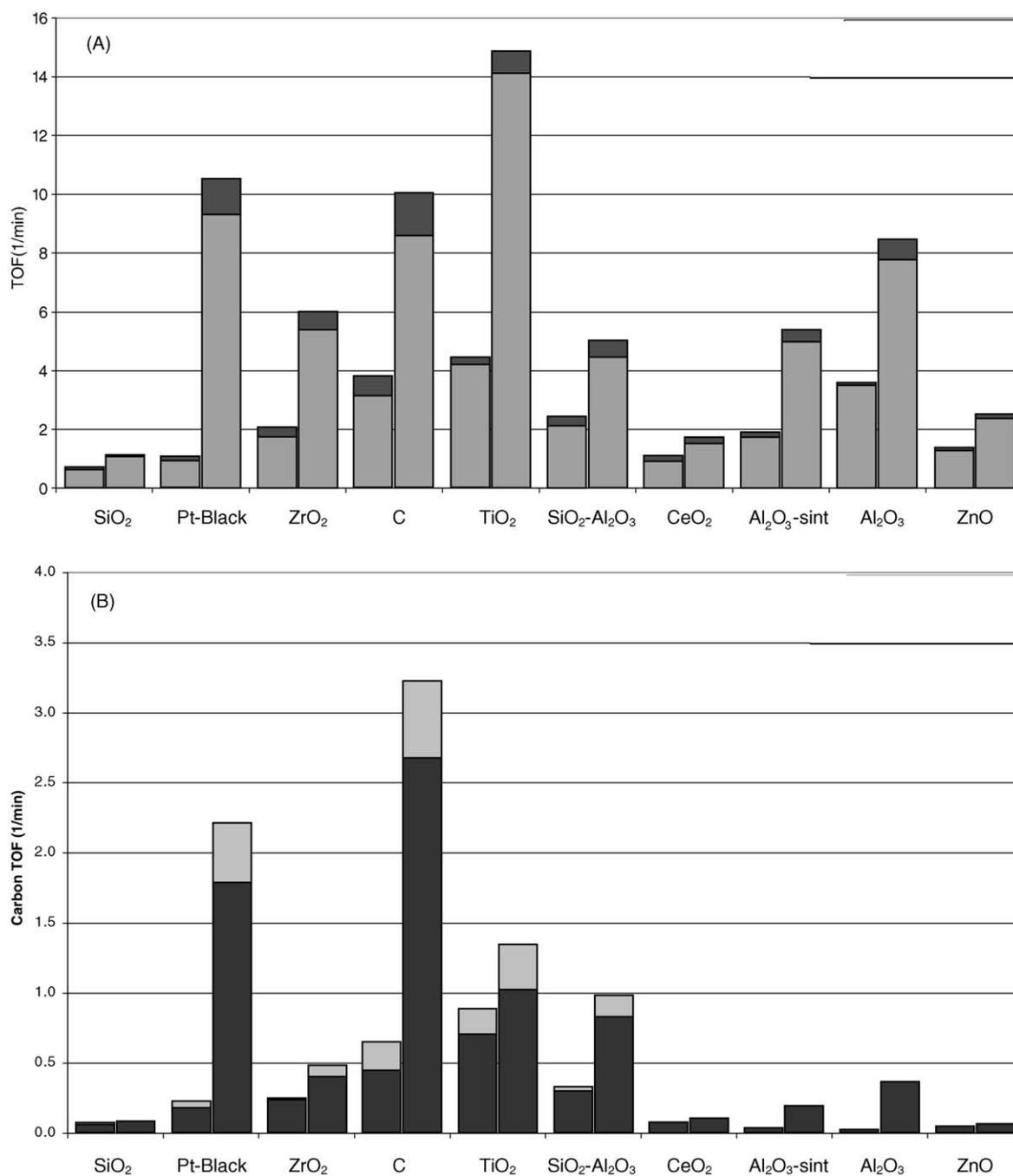


Fig. 5. Production rates for reforming of 10 wt.% aqueous ethylene glycol at 483 (left columns) and 498 K (right columns) over supported Pt catalysts. A) H<sub>2</sub> production rate (gray) and the amount of hydrogen that could be generated by total reforming of the methanol byproduct (black). B) Alkane production rate (methane and ethane) (gray) and production of alkane precursors (acetaldehyde, ethanol, and acetic acid) (black). Al<sub>2</sub>O<sub>3</sub>-sint indicates a Pt/Al<sub>2</sub>O<sub>3</sub> catalyst that has been subjected to treatment at elevated temperature in H<sub>2</sub>. Adapted from reference [10].

alumina-supported Pt catalysts at low conversion, and APR of both oxygenated hydrocarbons over Pt/Al<sub>2</sub>O<sub>3</sub> leads to nearly 100% selectivity for the formation of H<sub>2</sub> (compared to the formation of alkanes). Since the selectivity for hydrogen production from methanol and ethylene glycol is essentially independent of conversion, it appears that the series hydrogenation of CO/CO<sub>2</sub> to alkanes is not significant over Pt/Al<sub>2</sub>O<sub>3</sub>.

### 2.2.3. Reaction pathways

Fig. 6 shows a schematic representation of reaction pathways that we suggest are involved in the formation of H<sub>2</sub> and alkanes from an oxygenated hydrocarbon (e.g., ethylene glycol) over a metal catalyst. Ethylene glycol first undergoes reversible dehydrogenation steps to give adsorbed intermediates, prior to cleavage of C–C or C–O bonds. The adsorbed species can be formed on the metal surface either

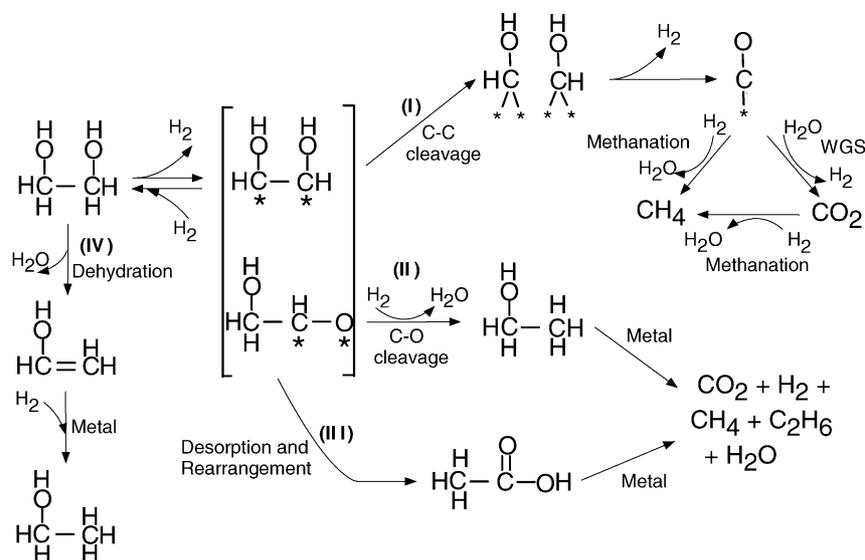


Fig. 6. Reaction pathways and selectivity challenges for production of H<sub>2</sub> from reactions of ethylene glycol with water (\* represents a surface metal site). Adapted from reference [8].

by formation of metal–carbon bonds and/or metal–oxygen bonds. On a metal catalyst such as platinum, the adsorbed species bonded to the surface by the formation of Pt–C bonds is more stable than the species involving Pt–O bonds [18]. However, Pt–O bonds may also be formed, since activation energy barriers for cleavage of O–H and C–H bonds are similar on Pt. Subsequent to formation of adsorbed species on the metal surface, three reaction pathways can occur, indicated as (I), (II) and (III) in Fig. 6. Pathway I involves cleavage of the C–C bond leading to the formation of CO and H<sub>2</sub>, followed by reaction of CO with water to form CO<sub>2</sub> and H<sub>2</sub> by the water-gas shift (WGS) reaction [17,24]. Further reaction of CO and/or CO<sub>2</sub> with H<sub>2</sub> (e.g., on metals such as Ni, Rh and Ru) leads to alkanes and water by methanation and Fischer–Tropsch reactions [12–15], and this degradation in the production of H<sub>2</sub> represents a series-selectivity challenge. Pathway II leads to the formation of an alcohol on the metal catalyst by cleavage of the C–O bond, followed by hydrogenation. The alcohol can undergo further reaction on the metal surface (adsorption, C–C cleavage, C–O cleavage) to form alkanes (CH<sub>4</sub>, C<sub>2</sub>H<sub>6</sub>), CO<sub>2</sub>, H<sub>2</sub> and H<sub>2</sub>O. This degradation in the production of H<sub>2</sub> (by alkane formation) represents a parallel-selectivity challenge. Pathway III involves desorption of species from the metal surface followed by rearrangement (which may occur on the catalyst support and/or in the aqueous phase) to form an acid, which can then undergo surface reactions (adsorption, C–C cleavage, C–O cleavage) to form alkanes (CH<sub>4</sub>, C<sub>2</sub>H<sub>6</sub>), CO<sub>2</sub>, H<sub>2</sub> and H<sub>2</sub>O. This pathway represents an additional parallel-selectivity challenge.

The catalyst support can affect the selectivity for H<sub>2</sub> production by catalyzing parallel dehydration pathways [25,26] that lead to the formation of alkanes. For example, the selectivity observed for the production of H<sub>2</sub> by APR of

ethylene glycol over silica-supported Pt is significantly lower than we have observed for APR over alumina-supported Pt [8,22]. Thus, it appears that the higher acidity of silica compared to alumina, as reflected by the lower isoelectric point of silica [27], can facilitate acid-catalyzed dehydration reactions of ethylene glycol, represented by pathway IV in Fig. 6, followed by hydrogenation on the metal surface to form an alcohol. The alcohol can subsequently undergo surface reactions, as in pathway II, to form alkanes (CH<sub>4</sub>, C<sub>2</sub>H<sub>6</sub>), CO<sub>2</sub>, H<sub>2</sub> and H<sub>2</sub>O. This bifunctional dehydration/hydrogenation pathway consumes H<sub>2</sub>, leading to decreased hydrogen selectivity and increased alkane selectivity.

#### 2.2.4. Nature of the feed

Experimental results for the APR of reforming of glucose, sorbitol, glycerol, ethylene glycol and methanol are illustrated in Fig. 7 [22]. Reactions were carried out over a Pt/Al<sub>2</sub>O<sub>3</sub> catalyst at 498 and 538 K. Fig. 7 indicates that the selectivity for H<sub>2</sub> production improves in the order glucose < sorbitol < glycerol < ethylene glycol < methanol. The figure also shows that lower operating temperatures result in higher H<sub>2</sub> selectivities, although this trend is in part due to the lower conversions achieved at lower temperatures. The selectivity for alkane production follows the opposite trend to that exhibited by the H<sub>2</sub> selectivity. The highest hydrogen yields are obtained when using sorbitol, glycerol and ethylene glycol as feed molecules for APR. Although these molecules can be derived from renewable feedstocks [28–31], the reforming of less reduced and more immediately available compounds such as glucose would be highly desirable. Unfortunately, as seen in Fig. 7, the hydrogen yield from APR of glucose is lower than for these other more reduced compounds. Furthermore, while the high hydrogen

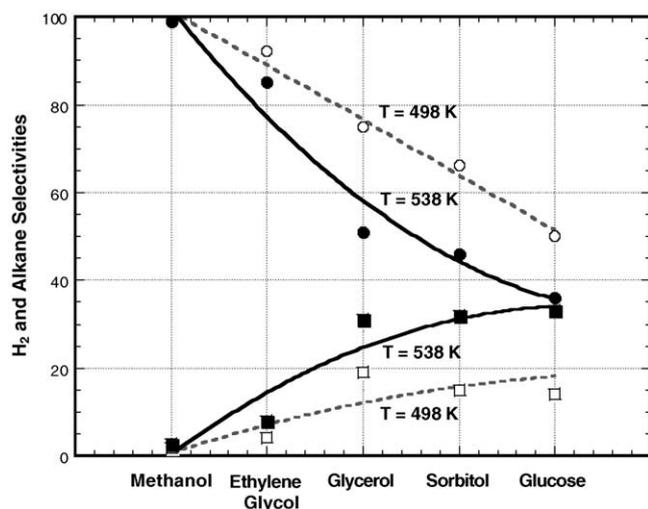


Fig. 7. Selectivities vs. oxygenated hydrocarbon. H<sub>2</sub> selectivity (circles) and alkane selectivity (squares) from aqueous-phase reforming of 1 wt.% oxygenated hydrocarbons over 3 wt.% Pt/Al<sub>2</sub>O<sub>3</sub> at 498 K (open symbols and dashed curves) and 538 K (filled symbols and solid curves). Adapted from reference [22].

yields for reforming of the polyols are insensitive to the concentration of the aqueous feed (e.g., from 1 to 10 wt.%), the hydrogen yield for reforming of glucose decreases further as the feed concentration increases to about 10 wt.%. The lower H<sub>2</sub> selectivities for the APR of glucose, compared to that achieved using the other oxygenated hydrocarbon reactants, are at least partially due to homogeneous reactions of glucose in the aqueous-phase at the temperatures employed in aqueous-phase reforming [32–35].

Reforming reactions are fractional order in the feed concentration [9], whereas glucose decomposition studies have shown first-order dependence on the feed concentration [34]. Thus, the rate of homogeneous glucose decomposition relative to the reforming rate increases with an increase in the glucose concentration from 1 to 10 wt.%. Accordingly, to collect the data presented in Fig. 7 [22], low concentrations (i.e., 1 wt.%) of all feed molecules were employed to minimize effects from homogeneous decomposition reactions and thereby compare the selectivities under conditions where the conversion of reactant is controlled by the Pt/Al<sub>2</sub>O<sub>3</sub> catalyst. This low feed concentration corresponds to a molar ratio H<sub>2</sub>O/C of 165. Processing such dilute solutions is economically not practical, even though reasonably high hydrogen yields are achieved. However, the undesirable homogeneous reactions observed with glucose pose less of a problem when using sorbitol, glycerol, ethylene glycol and methanol, which makes it possible to generate high yields of hydrogen by the APR of more concentrated solutions containing these compounds (e.g., aqueous solutions containing 10 wt.% of these oxygenated hydrocarbon reactants, corresponding to molar ratios H<sub>2</sub>O/C equal to 5).

### 2.3. Factors favoring production of heavier alkanes

Aqueous-phase reforming of sorbitol can be tailored to selectively produce a clean stream of heavier alkanes consisting primarily of butane, pentane and hexane. The conversion of sorbitol to alkanes plus CO<sub>2</sub> and water is an exothermic process that retains approximately 95% of the heating value and only 30% of the mass of the biomass-derived reactant. This reaction takes place by a bi-functional pathway involving first the formation of hydrogen and CO<sub>2</sub> on the appropriate metal catalyst (such as Pt) and the dehydration of sorbitol on a solid acid catalyst (such as silica–alumina) or a mineral acid. These initial steps are followed by hydrogenation of the dehydrated reaction intermediates on the metal catalyst. When these steps are balanced properly, the hydrogen produced in the first step is fully consumed by hydrogenation of dehydrated reaction intermediates, leading to the overall conversion of sorbitol to alkanes plus CO<sub>2</sub> and water. The selectivities for production of alkanes can be varied by changing the catalyst composition, the pH of the feed, the reaction conditions, and modifying the reactor design [36].

Fig. 8 shows the effect of increasing the solid or mineral acidity on the alkane selectivity. As solid acid (SiO<sub>2</sub>–Al<sub>2</sub>O<sub>3</sub>, containing 25 wt.% Al<sub>2</sub>O<sub>3</sub> from Grace Davison) is added to

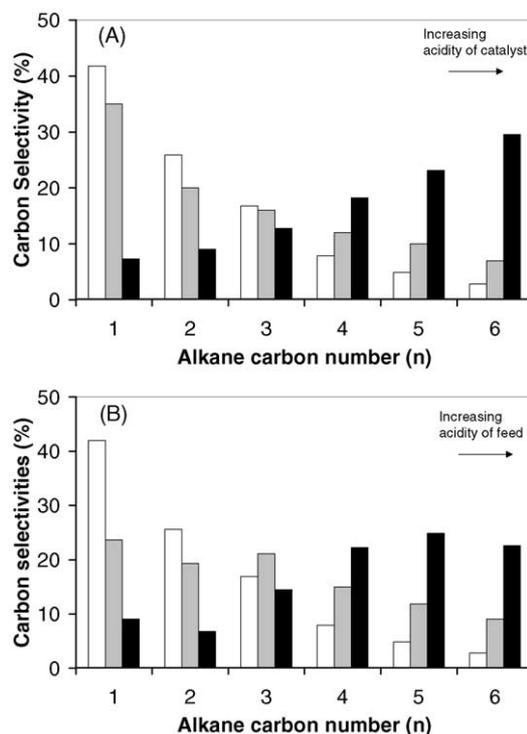


Fig. 8. Alkanes carbon selectivities for aqueous-phase reforming of 5 wt.% sorbitol at 538 K and 57.6 bar vs. A) addition of solid acid (SiO<sub>2</sub>–Al<sub>2</sub>O<sub>3</sub>) to 3 wt.% Pt/Al<sub>2</sub>O<sub>3</sub> [Pt/Al<sub>2</sub>O<sub>3</sub> (white), mixture 2: Pt/Al<sub>2</sub>O<sub>3</sub> (3.30 g) and SiO<sub>2</sub>–Al<sub>2</sub>O<sub>3</sub> (0.83 g), and mixture 1: Pt/Al<sub>2</sub>O<sub>3</sub> (1.45 g) and SiO<sub>2</sub>–Al<sub>2</sub>O<sub>3</sub> (1.11 g) (black)] and B) addition of mineral acid (HCl) in feed over 3 wt.% Pt/Al<sub>2</sub>O<sub>3</sub> [pH<sub>feed</sub> = 7 (white), pH<sub>feed</sub> = 3 (grey), and pH<sub>feed</sub> = 2 (black)]. Adapted from reference [36].

Pt/Al<sub>2</sub>O<sub>3</sub>, the selectivity to heavier alkanes increases, as shown in Fig. 8A. The alkanes formed are straight-chain compounds with only minor amounts of branched isomers (less than 5%). The H<sub>2</sub> selectivity decreases from 43 to 11% for the Pt/Al<sub>2</sub>O<sub>3</sub> catalyst upon adding the solid acid SiO<sub>2</sub>–Al<sub>2</sub>O<sub>3</sub>, indicating that the majority of the H<sub>2</sub> produced by the reforming reaction is consumed by the production of alkanes when the catalyst contains a sufficient number of acid sites. Similarly, the selectivity to heavier alkanes increases as a mineral acid (HCl) is added to the feed, as shown in Fig. 8B. The H<sub>2</sub> selectivity decreases from 43 to 6% as the pH of the feed decreases from 7 to 2.

A catalyst was prepared by depositing 4 wt.% Pt on the solid acid SiO<sub>2</sub>–Al<sub>2</sub>O<sub>3</sub> support [36], and this catalyst exhibited similar selectivity as the physical mixture of Pt/Al<sub>2</sub>O<sub>3</sub> with SiO<sub>2</sub>–Al<sub>2</sub>O<sub>3</sub>, for a similar ratio of Pt to solid acid sites [22]. The H<sub>2</sub> selectivity was usually less than 5% for the Pt/SiO<sub>2</sub>–Al<sub>2</sub>O<sub>3</sub>, indicating that most of the H<sub>2</sub> produced was consumed in the production of the alkanes. Changing the temperature of the reactor from 538 to 498 K had little effect on the product selectivity. In contrast, the hexane selectivity increases from 21 to 40% for the Pt/SiO<sub>2</sub>–Al<sub>2</sub>O<sub>3</sub> catalyst at 498 K as the pressure increases from 25.8 to 39.6 bar, indicating that the reaction conditions can be used to manipulate the alkane selectivity.

As another option to produce heavier alkanes by aqueous-phase reforming, H<sub>2</sub> can be co-fed to the reactor with the aqueous feed. When H<sub>2</sub> is co-fed with an aqueous solution containing 5 wt.% sorbitol over the Pt/SiO<sub>2</sub>–Al<sub>2</sub>O<sub>3</sub> catalyst at 498 K and 34.8 bar, the selectivity to pentane plus hexane increases from 55 to 78% [36]. Under these conditions, approximately 90% of the effluent gas phase carbon is present as alkanes. Accordingly, increasing the hydrogen partial pressure in the reactor increases the rate of hydrogenation compared to C–C bond cleavage on the metal catalyst surface. The co-feeding of H<sub>2</sub> with the aqueous feed allows bi-functional catalysts to be formulated using metals (such as Pd) that by themselves show low activities for hydrogen production by APR reactions. In this case the hydrogen required for the formation of alkanes by the bi-functional catalyst is supplied externally instead of being formed in the reactor by aqueous-phase reforming, and the sole role of the metal component is to catalyze hydrogenation reactions.

#### 2.4. Producing hydrogen containing low levels of CO: ultra-shift

Production of hydrogen containing low levels of CO is critical for energy generation using hydrogen PEM fuel cells. Aqueous-phase reforming of oxygenates takes place over metal catalysts to produce CO and H<sub>2</sub>. Adsorbed CO undergoes water-gas shift, which increases the amount of H<sub>2</sub> produced and removes CO from the catalyst surface [37]. The lowest partial pressure of CO that can be achieved depends on the thermodynamics of the water-gas shift

reaction and the operating conditions as given by:

$$P_{\text{CO}} = \frac{P_{\text{CO}_2} P_{\text{H}_2}}{K_{\text{WGS}} P_{\text{H}_2\text{O}}}$$

where  $K_{\text{WGS}}$  is the equilibrium constant for the vapor-phase water-gas shift and  $P_j$  the partial pressures. Since H<sub>2</sub>, CO<sub>2</sub>, and small amounts of alkanes (primarily CH<sub>4</sub>) are produced by APR, gas bubbles are formed within the liquid-phase flow reactor. As noted above with respect to the effects of system pressure on reaction kinetics, the pressure in these bubbles can be approximated to be equal to the system pressure. Accordingly, the partial pressures of water vapor and the reaction products are dictated by the feed concentrations, system pressure and temperature, as outlined below [38].

For dilute product concentrations and system pressures above the saturation pressure of water, gaseous bubbles contain water vapor at a pressure equal to its saturation pressure at the reactor temperature, and the remaining pressure is the sum of the partial pressures of the product gases. The extent of vaporization,  $y$ , is defined as the percent of water in the vapor phase relative to the total amount of water flowing in the reactor. In contrast, for systems operated at pressures that are near the saturation pressure of water, all the liquid water may vaporize and the composition of the bubble is dictated by the stoichiometry of the feed stream. At this condition, the partial pressure of water is below its saturation pressure because the water vapor is diluted by the reforming product gases. Higher concentrations of ethylene glycol lead to lower partial pressures of water because of greater dilution from H<sub>2</sub> and CO<sub>2</sub> produced by reforming reactions. As the system pressure is increased, the partial pressure of water vapor increases until it reaches the saturation pressure of water, at which point any further increase in the system pressure leads to partial condensation of liquid water.

The above arguments indicate that the conditions which favor the lowest levels of CO from reforming of oxygenates are those which lead to the lowest partial pressures of H<sub>2</sub> and CO<sub>2</sub> in the reforming gas bubbles; and, these conditions are achieved by operating at system pressures that are near the saturation pressure of water and at low ethylene glycol feed concentrations. As the system pressure increases and extent of vaporization decreases below 100%, the partial pressures of H<sub>2</sub> and CO<sub>2</sub> in the bubble increase, thereby leading to higher equilibrium concentrations of CO. Similarly, as the ethylene glycol concentration in the feed increases, higher partial pressures of H<sub>2</sub> and CO<sub>2</sub> are developed, even for the case of complete vaporization, again leading to higher equilibrium CO concentrations.

Fig. 9 shows the results for APR of 2 wt.% ethylene glycol over a Pt/Al<sub>2</sub>O<sub>3</sub> catalyst contained in an upflow reactor, which was divided into two separately heated reaction zones [38]. Reforming reactions were carried out in the lower section (denoted as the reforming-zone), maintained at 498 K. The temperature of the top section (denoted as the shift-zone), system pressure, feed concentration, and

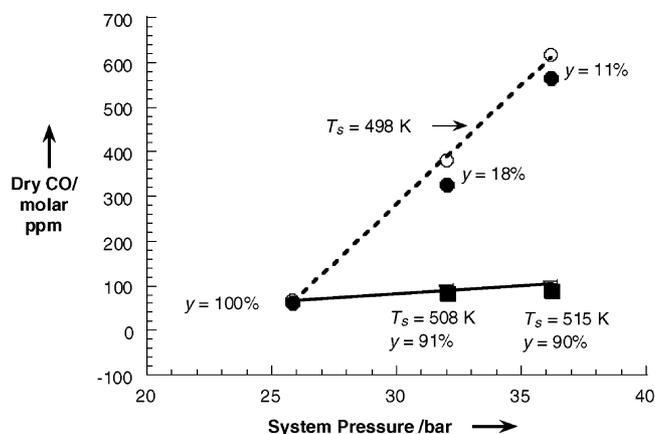


Fig. 9. Effect of process variables on CO concentration for 2% EG. Circles: CO concentration vs. system pressure at shift temperature  $T_s = 498$  K, squares: ultra-shift at higher shift temperatures. Open symbols represent equilibrium CO and filled symbols represent observed CO. Adapted from reference [38].

feed flow rate were variables of the system. The observed CO concentration in the effluent gas and the corresponding equilibrium concentration are reported in Fig. 9 for system pressures of 25.8, 32.0 and 36.2 bar, with the shift-zone of the reactor maintained at the same temperature as the reforming temperature of 498 K. Since the saturation pressure of water at 498 K is equal to 25.1 bar, liquid water is completely vaporized at a system pressure of 25.8 bar and the  $H_2$  pressure in the bubble is calculated to be 0.77 bar, leading to a low equilibrium CO concentration of 66 ppm in the reactor effluent. At system pressures of 32 and 36.2 bar, the  $H_2$  pressures are 4.60 and 7.53 bar, respectively, with only 18 and 11% vaporization of water occurring in each case. These conditions lead to higher equilibrium CO concentrations of 380 and 617 ppm, respectively.

Although the lowest levels of CO are obtained when the reactor is operated near the saturation pressure of water, this condition is not feasible for larger, non-volatile feeds such as glucose, which undergo undesirable decomposition reactions when vaporized [32–35]. It thus becomes imperative to operate the reformer at system pressures above the saturation pressure of water, to maintain liquid phase conditions. In these cases, we propose a process, which we denote as ‘ultra-shift’, to achieve very low levels of CO in the product gas from APR of oxygenated hydrocarbons, conducted at pressures above the saturation pressure of water. This process involves vaporization of liquid water (in the shift-zone) to dilute the  $H_2$  and  $CO_2$  in the bubbles, thereby favoring increased conversion of the water-gas shift reaction and leading to lower CO concentrations.

The feasibility of the ultra-shift process is depicted in Fig. 9 [38]. It is seen that at a system pressure of 32 bar, when the temperature of the shift-zone was increased from 498 to 508 K, 91% of the water in this zone vaporized, thereby decreasing the  $H_2$  pressure to 1.05 bar, and lowering

the measured CO concentration from 380 to 84 ppm. In the case where the system pressure was 36.2 bar, increasing the temperature of the shift-zone from 498 to 515 K decreased the  $H_2$  pressure from 7.53 to 1.14 bar and the measured CO concentration from 564 to 89 ppm. At the higher temperatures, the effect of diluting the  $H_2$  and  $CO_2$  pressures with water vapor supersedes the less favorable thermodynamics, leading to ultra-shift.

## 2.5. Hydrogen from concentrated glucose feeds

Aqueous-phase reforming of glucose ( $C_6O_6H_{12}$ ) is of particular interest for biomass utilization, because this sugar comprises the major energy reserves in plants and animals. As discussed earlier, the hydrogen selectivity from reforming of glucose decreases as the liquid concentration increases from 1 to 10 wt.% because of undesired hydrogen-consuming side reactions that occur in the liquid phase [34]. This decrease in selectivity is an important limitation, because processing dilute aqueous solutions involves the processing of excessive amounts of water.

Fig. 10 depicts various reaction pathways that take place during APR of glucose and sorbitol [39]. Production of  $H_2$  and  $CO_2$  from glucose (G) and sorbitol (S) takes place on metal catalysts such as Pt or Ni–Sn alloys (pathways G1 and S1) via cleavage of C–C bonds followed by water-gas shift. As discussed earlier, undesired alkanes can be formed by cleavage of C–O bonds on the metal catalyst and dehydration processes on acidic catalyst supports (pathways G2, S2). In the case of glucose, undesired reactions can also take place in the aqueous phase to form organic acids, aldehydes and carbonaceous deposits (pathway G3). These undesirable homogeneous decomposition reactions are first order in the glucose concentration, whereas the desirable reforming reactions on the catalyst surface are fractional order; therefore, high concentrations of glucose lead to low hydrogen selectivities. The hydrogenation of glucose to sorbitol (pathway G–S) also takes place on metal catalysts with high selectivity at low temperatures (e.g., 400 K) and high  $H_2$  pressures.

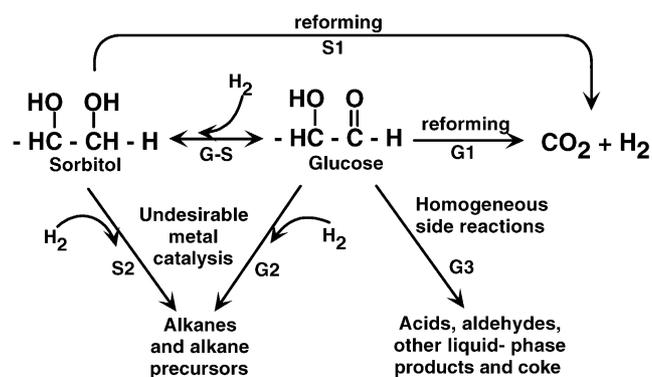


Fig. 10. Reaction pathways involved in glucose and sorbitol reforming. Adapted from reference [39].

The rates of pathways G1, G2 and G3 increase more rapidly with temperature than does the rate of pathway G–S. Accordingly, a strategy for improving the hydrogen selectivity from APR of glucose is to employ a dual-reactor system involving a low-temperature hydrogenation step followed by a higher-temperature reforming process. In this respect, we have conducted studies in which the partial pressures of the gas phase products in the reactor were varied by co-feeding a gas stream ( $N_2$  or  $H_2$ ) with the liquid feed (10 wt.% glucose/sorbitol) at the inlet of the reactor. The performance of the reactor in this mode can be then compared to the case where only liquid was fed to the reactor and  $N_2$  sweep gas was combined with the effluent stream at the exit of the reactor. It was found that the hydrogen selectivities observed for APR of glucose ( $\sim 10$ – $13\%$ ) were much lower compared to reforming of sorbitol ( $\sim 60\%$ ) under similar conditions. Also higher alkane selectivities of 47–50% were observed for reforming of glucose, indicating that APR of glucose, even with hydrogen co-fed with the liquid reactant stream at the inlet of the reactor, is not selective for production of  $H_2$ . These results indicate that co-feeding hydrogen with liquid reactants into the reforming reactor at 538 K (and 52.4 bar) does not lead to rapid hydrogenation of glucose into sorbitol and its subsequent reforming to give high  $H_2$  selectivities. Similarly, sorbitol does not undergo rapid dehydrogenation to glucose under conditions of APR where  $H_2$  is not co-fed with the liquid reactant stream to the reforming reactor, a desirable result.

Experiments were conducted by co-feeding gaseous  $H_2$  with aqueous solutions containing 10 wt.% sorbitol or glucose into a dual-reactor system consisting of a hydrogenation reactor at 393 K followed by a reforming reactor at 538 K [39]. The presence of the hydrogenation reactor did not affect the APR of sorbitol. However, when

10 wt.% glucose was co-fed with gaseous  $H_2$  to the dual-reactor system, then high hydrogen selectivity (62.4%) and low alkane selectivity (21.3%) were obtained, these values being similar to the selectivities obtained from the reforming of sorbitol. These results indicate that glucose is first completely hydrogenated to sorbitol before being sent to the reformer in which the sorbitol is then converted with high selectivity to  $H_2$  and  $CO_2$ .

### 3. Discussion and overview

Fig. 11 summarizes the thermodynamic and kinetic aspects that form the foundation of the APR process. In contrast to alkane reforming which is favorable only at high temperatures, the reforming of oxygenated hydrocarbons (C:O ratio of 1:1) to form  $CO$  and  $H_2$  is thermodynamically favorable at relatively lower temperatures of 400 K. Also, the subsequent water-gas shift reaction, necessary to convert the carbon monoxide generated by reforming to carbon dioxide, becomes increasingly favorable at lower temperatures. In addition, results from DFT calculations indicate that the activation energy required to break the C–C bond in oxygenated hydrocarbons is lower than that required for alkanes, indicating that C–C cleavage is easier in oxygenates than in alkanes. These results suggest that it is possible to design a process in which oxygenated hydrocarbons can be converted to  $H_2$  and  $CO_2$  in a single-step process, wherein both the reforming and water-gas shift reactions are conducted in the same low-temperature reactor. Although the more volatile oxygenates such as methanol, ethylene glycol and glycerol can be processed in the vapor as well as liquid phases, processing less volatile oxygenates such as glucose and sorbitol under vapor-phase conditions would

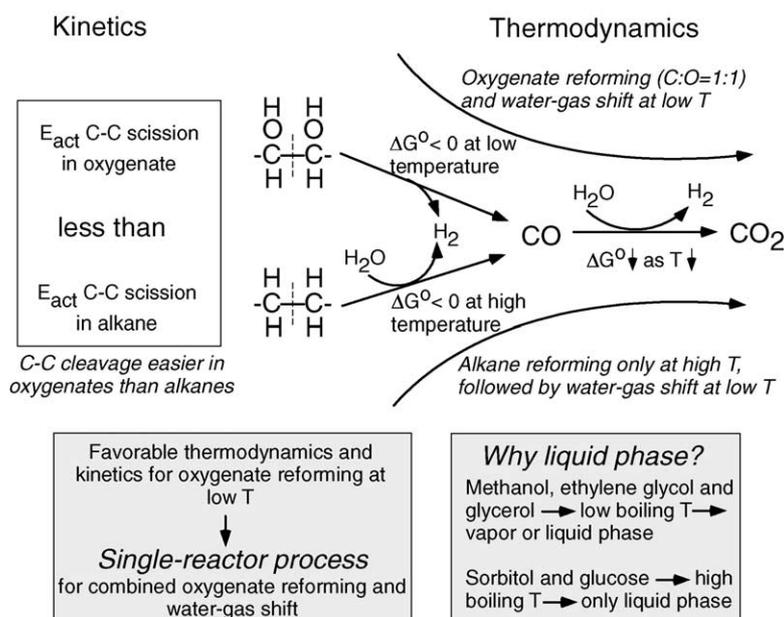


Fig. 11. Summary of thermodynamic and kinetic considerations that form the basis of the aqueous-phase reforming process.

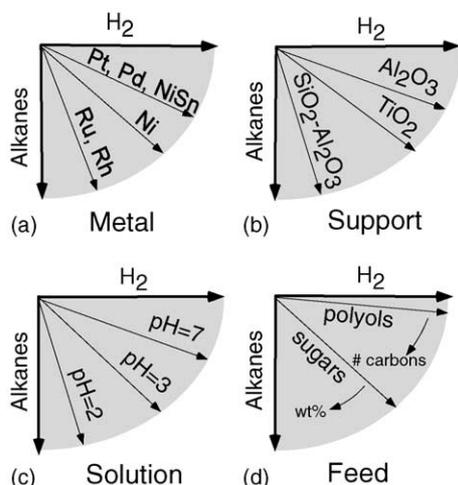


Fig. 12. Factors controlling the selectivity of the aqueous-phase reforming process.

require high-temperature reforming, followed by water-gas shift at lower temperatures, thus obviating the advantages of a single-reactor low-temperature process.

Fig. 12 summarizes the effects of various factors on the selectivity of hydrogen production, and also suggests process conditions that may lead to the selective production of alkanes, if desired, from oxygenated hydrocarbons. It is seen from Fig. 12a, that metals such as Pt, Pd and Ni–Sn alloys show high selectivity for hydrogen production and very low tendency for formation of alkanes. In comparison, supported Ni catalysts tend to make more alkanes and also show some deactivation with time, which may be due to sintering of the metal particles, leading to lower dispersions. Fig. 12a also shows that metals such as Ru and Rh are very active for alkane formation and make very little hydrogen.

The support plays an important role in the selectivity of the APR process, as summarized in Fig. 12b. The more acidic supports (e.g., silica–alumina) lead to high selectivities for alkane formation, whereas the more basic/neutral supports (e.g., alumina) favor hydrogen production. Supports with mild acidity fall within the spectrum of the two extremes, as seen for titania-based catalysts. The acidity of the solution also affects the performance of the aqueous-phase reformer in a similar way. Depending on the nature of the byproduct/intermediate compounds formed in the reactor, the aqueous solution in contact with the catalyst can be acidic, neutral or basic. Also gaseous carbon dioxide dissolved in the solution at high pressures makes a slightly acidic solution (pH = 4–5). Acidic solutions (pH = 2–4) promote alkane formation, due to acid-catalyzed dehydration reactions that occur in solution (followed by hydrogenation on the metal). In contrast, neutral and basic solutions lead to high hydrogen selectivities and low alkane selectivities, as shown in Fig. 12c.

The type of feed also has a strong influence on the reaction selectivity. In general, polyols (e.g., sorbitol) have a higher selectivity for H<sub>2</sub> production than sugars (e.g.,

glucose). Within the family of polyols, the hydrogen selectivity decreases with increasing carbon number of the feed, probably because the number of undesired hydrogen-consuming side reactions increases accordingly. Also, processing higher feed concentrations of glucose leads to lower hydrogen selectivities. For example, as the glucose feed concentration increases from 1 to 10 wt.%, the alkane selectivity increases from 30 to 50%, and the hydrogen selectivity decreases accordingly. This change with concentration is caused by undesired homogeneous decomposition reactions associated with sugars. These different feed effects have been summarized in Fig. 12d.

Fig. 13 outlines the various reaction pathways that can take place in the APR reactor (for polyols as feed), resulting in multiple selectivity challenges. The oxygenated hydrocarbon feedstock can undergo reforming via C–C cleavage on the metal surface to make the desired H<sub>2</sub> and CO<sub>2</sub>. The CO<sub>2</sub> formed can undergo undesired series methanation/Fischer–Tropsch synthesis reactions to form alkanes. Alternately, some metals have a tendency to favor C–O bond scission, followed by hydrogenation to make alcohol intermediates, which can then further react on the metal surface (C–C/C–O cleavage) to form alkanes. These reactions constitute parallel-selectivity challenges on the

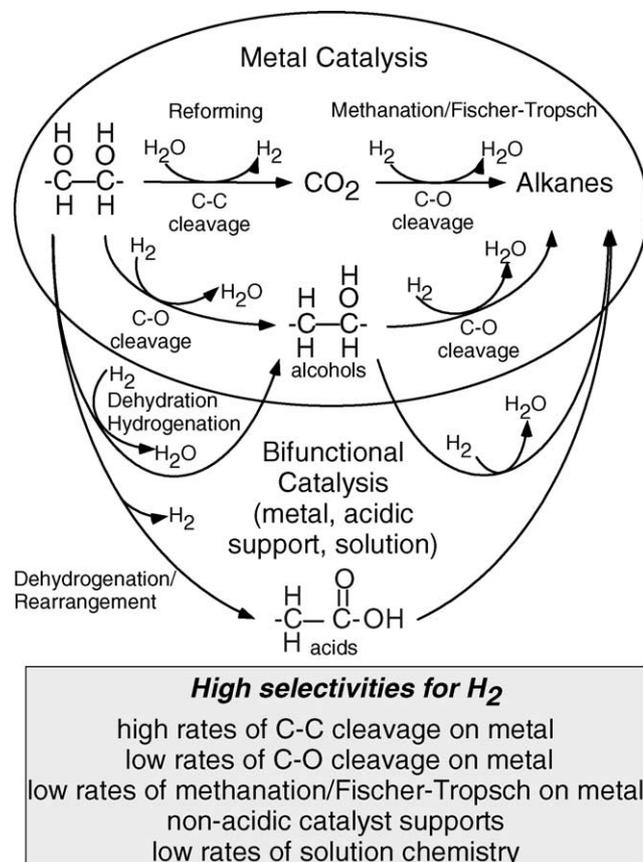


Fig. 13. Summary of reaction pathways involved in the aqueous-phase reforming of oxygenated hydrocarbons leading to multiple selectivity challenges.

metal surface. In addition to metal catalyzed reactions, undesired bi-functional catalysis can occur by combinations of metal, support and solution, as shown in Fig. 13. Reaction pathways such as dehydration–hydrogenation leading to alcohols, and dehydrogenation–rearrangement to form acids can occur in solution or on the support aided by metal catalysis. These intermediates can then react further in solution or on the catalyst to make more alkanes. To obtain high selectivities for hydrogen production, the metal catalyst should show high rates of C–C cleavage, low rates of C–O cleavage and low rates of series methanation/Fischer–Tropsch synthesis reactions. Metals such as Pt and Ni–Sn alloy systems show these favorable characteristics. Also the support should not favor dehydration/C–O cleavage reactions or promote the formation of acids in aqueous solution. Acidic supports such as silica–alumina have shown a tendency to promote these undesirable reactions. Hence, non-acidic supports such as alumina are required to obtain high selectivities for hydrogen production via APR reactions. Finally, acidic solutions also lead to dehydration of the feed polyol, which ultimately leads to alkane formation.

Low CO levels in the product gas can be obtained by operating at suitable reaction conditions. Fig. 14 outlines the concept of the ultra-shift process used to drive the CO levels to as low as possible. Based on the water-gas shift equilibrium, the partial pressure of CO ( $P_{CO}$ ) in the reactor is proportional to the partial pressure of hydrogen ( $P_{H_2}$ ), which in turn decreases as the partial pressure of water ( $P_{water}$ ) in the system approaches the total system pressure ( $P_{total}$ ). Thus, to reduce the equilibrium concentration of CO in the reactor, the hydrogen pressure should be lowered by increasing the water pressure in the system. This effect can be achieved using the ultra-shift process, wherein the water

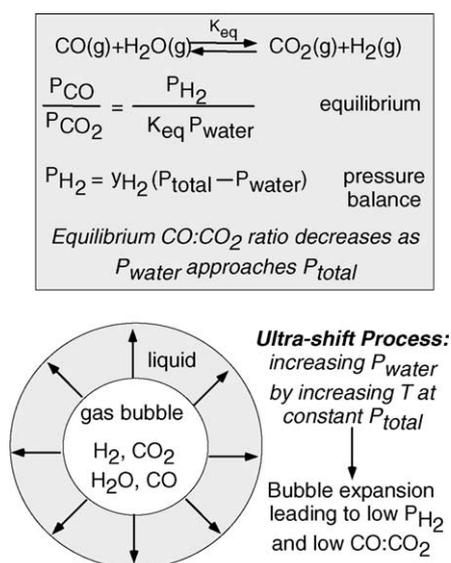


Fig. 14. Concept of the ultra-shift process for obtaining low CO levels in the product gas.

pressure is increased either by reducing the system pressure in an isothermal reactor, or increasing the temperature of the upper ultra-shift-zone of the isobaric reactor. For example, when the shift temperature is maintained at the reforming temperature of 498 K, the effluent concentration of CO increases as the system pressure is increased. However, when the shift temperature is increased such that a majority of the liquid water vaporizes, then the product CO concentration, even at the higher pressures, decreases to below 100 ppm for 2% ethylene glycol. Thus, the addition of the ultra-shift-zone to the reforming reactor leads to low CO levels while allowing for processing of non-volatile feedstocks such as glucose in the lower aqueous-phase reformer. Importantly, when the effluent from the reactor is subsequently cooled to condense liquid water, then the pressure of the non-condensable gases increases and approaches the system pressure. This process of ultra-shift, involving initial vaporization followed by condensation of liquid water, thus leads to the desirable production of fuel-cell-grade  $H_2$  at high pressures and containing very low levels of CO.

The basis for the dual-reactor process for handling concentrated glucose feeds is summarized in Fig. 15. One of the important limitations of the APR of glucose solutions is that the hydrogen selectivity decreases when higher concentration feeds are used. This limitation is specific to glucose feedstocks, and a sugar–alcohol such as sorbitol does not suffer this restriction. Starting with glucose, the main desirable reaction that can occur is the catalytic reforming at high temperatures to form  $H_2$  and  $CO_2$ . In addition, undesired homogeneous decomposition reactions can occur at the same reaction conditions as reforming, to produce alkanes and coke. The rate of reforming increases

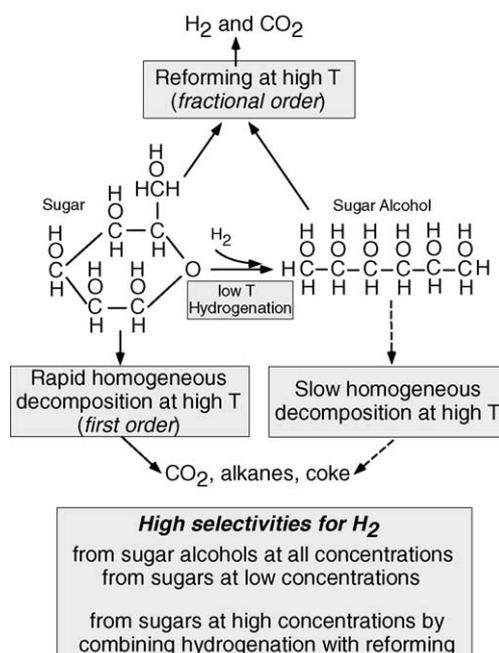


Fig. 15. Basis for the dual-reactor system employed in the processing of concentrated glucose feedstocks.

more slowly with increasing feed concentration, as compared to the decomposition rates, leading to lower hydrogen selectivities at higher feed concentrations. Also, glucose can undergo hydrogenation (using  $H_2$  produced by reforming or supplied externally) to form sorbitol, which can then undergo reforming on the catalyst surface to produce the desired  $H_2$  and  $CO_2$ . Since sorbitol decomposition rates in aqueous solution are much slower relative to the sorbitol reforming rates, high hydrogen selectivities can be obtained at all concentrations of the feed. The activation energy barrier for glucose hydrogenation is lower than the activation energies for glucose reforming and glucose decomposition. Therefore, glucose hydrogenation becomes dominant at lower temperatures, and almost complete conversion of glucose to sorbitol can be achieved, without any conversion to  $H_2$  and  $CO_2$ . The relative rates of the different reactions involved in glucose processing thus indicate that for the efficient extraction of hydrogen from glucose feedstocks, it is necessary to utilize an initial hydrogenation reactor that converts the glucose to sorbitol, followed by a reforming reactor to produce hydrogen with high selectivities, as described in Fig. 15.

We now outline how the APR process can be manipulated to obtain a product with the desired specifications. Sugar alcohols such as sorbitol give higher hydrogen selectivities than the corresponding sugar, i.e., glucose. Thus polyols (including sugar-alcohols) can be processed directly in the aqueous-phase reformer to obtain relatively high hydrogen selectivities, without any upstream processing. However, as shown in Fig. 16, co-feeding hydrogen with the aqueous feed

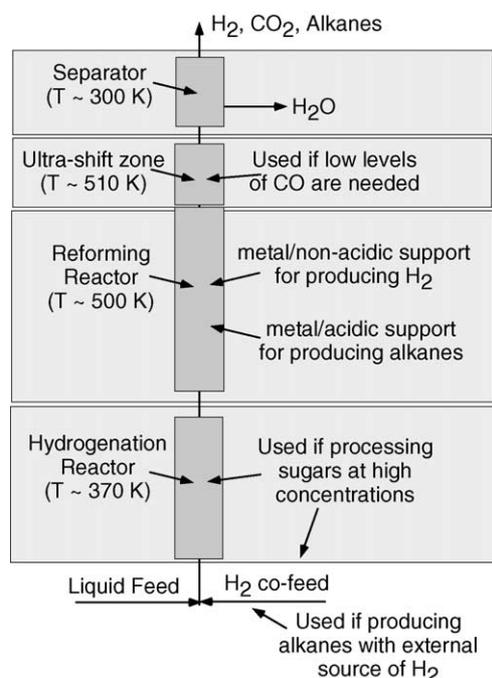


Fig. 16. Summary of the process conditions employed to obtain a product of the desired specifications using the aqueous-phase reforming process.

and employing a low-temperature hydrogenation reactor upstream from the reformer are used for processing sugars at high concentrations to obtain hydrogen in high selectivities. To obtain alkanes from concentrated sugars, a similar hydrogenation to sorbitol is first carried out, followed by reaction over an acidic catalyst in the presence of a hydrogen co-feed. For applications such as PEM fuel cells wherein very low levels of CO in the hydrogen fuel are necessary for efficient operation, an ultra-shift-zone, downstream of the reformer may be used to lower the outlet CO levels in the gas.

A novel aspect of the APR process is that a beneficial synergy is formed by operating the hydrogenation reactor, the reforming reactor, the ultra-shift-zone of the reactor, and the gas-liquid separator (situated downstream of the reactors) at different temperatures while maintaining the total pressure of the system at a constant value, as depicted schematically in Fig. 16. An aqueous solution of glucose can be co-fed with gaseous  $H_2$  to the hydrogenation reactor, which is operated at a relatively low temperature ( $T \sim 370$  K) to minimize glucose decomposition reactions in the liquid phase. At the low vapor pressure of water corresponding to this hydrogenation temperature, the partial pressure of hydrogen in this reactor is high, and hence favorable for the conversion of glucose to sorbitol. The aqueous solution of sorbitol and gaseous  $H_2$  are then fed to the reforming (or alkane formation) reactor, which is operated at the higher temperature ( $T \sim 500$  K), necessary to convert sorbitol to  $H_2$  and  $CO_2$  (or alkanes). If low levels of CO are required in the product gas, an ultra-shift-zone ( $T \sim 510$  K) downstream of the reforming reactor can be employed. Finally, the liquid and gaseous effluents from the reactor are cooled and sent to a separator, which is maintained at a low temperature ( $T \sim 300$  K), and the sum of the  $H_2$  and  $CO_2$  (or alkanes) pressures is essentially equal to the total pressure of the system. In the case of a hydrogen-rich reformat, this high pressure facilitates further removal of  $CO_2$  from  $H_2$  by pressure-swing adsorption or membrane separation. A fraction of the purified  $H_2$  at high pressure can then be recycled to the hydrogenation reactor, and the remaining hydrogen may be directed to a fuel cell for generation of electrical power.

An important advantage of the APR process is that it can be tailored to make renewable fuels such as  $H_2$  or alkanes in high selectivity. Another advantageous consequence of making  $H_2$  and alkanes via the APR process is that the energy required for the endothermic reforming of oxygenates may be produced internally, by allowing a fraction of the oxygenated compound to form alkanes through exothermic reaction pathways. In this respect, the formation of a mixture of hydrogen and alkanes from APR of oxygenates may be essentially neutral energetically, and little additional energy is required to drive the reaction. The gas effluent from the reformer could then be utilized as a feed to an internal combustion engine or suitable fuel cell (such as a solid oxide fuel cell).

#### 4. Conclusions

Aqueous-phase reforming of biomass-derived oxygenated hydrocarbons is a new process to produce renewable fuels consisting of hydrogen and alkanes. Catalysts based on Pt and Ni–Sn alloys are promising materials for hydrogen production. Various competing reaction pathways are involved in the reforming process, leading to parallel and series-selectivity challenges for production of hydrogen. The selectivity of the reforming process depends on various factors such as nature of the catalytically active metal, support, solution pH, feed and process conditions. By manipulating these factors, the APR process can be tailored to produce either H<sub>2</sub> or alkanes. Moreover, the molecular weight distribution of the alkane product stream can also be controlled, for example, to favor the formation of heavier alkanes using bi-functional catalysts containing metal and acidic components. Also, it is possible to operate the APR process to achieve very low CO levels in the product by using an ultra-shift-zone downstream of the reactor. Aqueous-phase reforming is best conducted using polyol feed molecules (e.g., sorbitol), because the product distribution obtained is relatively insensitive to the aqueous feed concentration (e.g., from 1 to 10 wt.%, and probably higher). In contrast, processing high concentrations of sugars (e.g., glucose) is accompanied by undesirable decomposition reactions. However, in these cases, a dual-reactor approach can be used for processing high concentrations of glucose, in which glucose is hydrogenated to sorbitol in the first reactor, and sorbitol is passed to the APR reactor for selective production of hydrogen or alkanes.

We note, in closing, that aqueous-phase reforming is a remarkably flexible process that can be tailored to selective produce hydrogen or to produce an alkane stream with a desired molecular weight distribution. Accordingly, this process offers exciting research opportunities for developing new generation of heterogeneous catalysts using metals, metal alloys, supports, and promoters that are stable under aqueous-phase reaction conditions.

#### Acknowledgements

This work was supported by the U.S. Department of Energy (DOE), Office of Basic Energy Sciences, Chemical Science Division, and by the National Science Foundation (NSF) through a STTR grant. Funding has also been provided by Conoco-Phillips and by Daimler-Chrysler. We would like to thank Kyle Allen, Dan Current, Andrew Richardson, Bret Wagner, Jonathan Tomshine, David Wishnik, Sibongile Nkosi, Dante Simonetti, Nicole Otto, Juben Chheda, Nitin Agarwal and Shampa Kandoi for assistance in catalyst preparation and reaction kinetic measurements, Marco Sanchez-Castillo and Joseph Napier

for assistance with analysis of reaction products. We also thank Manos Mavrikakis for valuable discussions.

#### References

- [1] J.R. Rostrup-Nielsen, *Steam Reforming Catalysts*, Danish Technical Press, Copenhagen, 1975.
- [2] J. Rostrup-Nielsen, *Phys. Chem. Chem. Phys.* 3 (2001) 283.
- [3] J. Woodward, M. Orr, K. Cordray, E. Greenbaum, *Nature* 405 (2000) 1014.
- [4] L. Garcia, R. French, S. Czernik, E. Chornet, *Appl. Catal. A Gen.* 201 (2000) 225.
- [5] K. Belkacemi, G. Turcotte, P. Savoie, *Ind. Eng. Chem. Res.* 41 (2002) 173.
- [6] S. Czernik, R. French, S. Feik, E. Chornet, *Ind. Eng. Chem. Res.* 41 (2002) 4209.
- [7] S.E. Jacobsen, C.E. Wyman, *Ind. Eng. Chem. Res.* 41 (2002) 1454.
- [8] R.R. Davda, J.W. Shabaker, G.W. Huber, R.D. Cortright, J.A. Dumesic, *Appl. Catal. B Environ.* 43 (2002) 13.
- [9] J.W. Shabaker, G.W. Huber, R.R. Davda, R.D. Cortright, J.A. Dumesic, *J. Catal.* 215 (2003) 344.
- [10] J.W. Shabaker, G.W. Huber, R.R. Davda, R.D. Cortright, J.A. Dumesic, *Catal. Lett.* 88 (2003) 1.
- [11] G.W. Huber, J.W. Shabaker, J.A. Dumesic, *Science* 300 (2003) 2075.
- [12] R.S. Dixit, L.L. Taviarides, *Ind. Eng. Chem. Process. Des. Dev.* 22 (1983) 1.
- [13] E. Iglesia, S.L. Soled, R.A. Fiato, *J. Catal.* 137 (1992) 212.
- [14] C.S. Kellner, A.T. Bell, *J. Catal.* 70 (1981) 418.
- [15] M.A. Vannice, *J. Catal.* 50 (1977) 228.
- [16] J.H. Sinfelt, D.J.C. Yates, *J. Catal.* 8 (1967) 82.
- [17] D.C. Grenoble, M.M. Estadt, D.F. Ollis, *J. Catal.* 67 (1981) 90.
- [18] R. Alcalá, M. Mavrikakis, J.A. Dumesic, *J. Catal.* 218 (2003) 178.
- [19] B. Lindstrom, L.J. Pettersson, *Int. J. Hydrogen Energy* 26 (2001) 923.
- [20] G.A. Somorjai, *Introduction to Surface Chemistry and Catalysis*, Wiley, New York, 1994.
- [21] R.R. Davda, R. Alcalá, J. Shabaker, G. Huber, R.D. Cortright, M. Mavrikakis, J.A. Dumesic, *Stud. Surf. Sci. Catal.* 145 (2003) 79.
- [22] R.D. Cortright, R.R. Davda, J.A. Dumesic, *Nature* 418 (2002) 964.
- [23] J.W. Shabaker, G.W. Huber, J.A. Dumesic, *J. Catal.* 222 (2004) 180.
- [24] S. Hilaire, X. Wang, T. Luo, R.J. Gorte, J. Wagner, *Appl. Catal. A Gen.* 215 (2001) 271.
- [25] S.P. Bates, R.A. Van Santen, *Adv. Catal.* 42 (1998) 1.
- [26] B. Gates, *Catalytic Chemistry*, Wiley, New York, 1992.
- [27] G.A. Parks, *Chem. Rev.* 65 (1965) 177.
- [28] H. Li, W. Wang, J.F. Deng, *J. Catal.* 191 (2000) 257.
- [29] B. Blanc, A. Bourrel, P. Gallezot, T. Haas, P. Taylor, *Green Chem.* 2 (2000) 89.
- [30] R. Narayan, G. Durrence, G.T. Tsao, *Biotech. Bioeng. Symp.* 14 (1984) 563.
- [31] E. Tronconi, N. Ferlazzo, P. Forzatti, I. Pasquon, B. Casale, L. Marini, *Chem. Eng. Sci.* 47 (1992) 2451.
- [32] G. Eggleston, J.R. Vercellotti, *J. Carbohydr. Chem.* 19 (2000) 1305.
- [33] B.M. Kabyemela, T. Adschiri, R.M. Malaluan, K. Arai, *Ind. Eng. Chem. Res.* 36 (1997) 1552.
- [34] B.M. Kabyemela, T. Adschiri, R.M. Malaluan, K. Arai, *Ind. Eng. Chem. Res.* 38 (1999) 2888.
- [35] A.R. Sapronov, *Khlebopek. Konditer. Prom.* 13 (1969) 12.
- [36] G.H. Huber, R.D. Cortright, J.A. Dumesic, *Angew. Chem. Int. Ed.* 43 (2004) 1549.
- [37] J. Novakova, L. Kubelkova, *Appl. Catal. B Environ.* 14 (1997) 273.
- [38] R.R. Davda, J.A. Dumesic, *Angew. Chem. Int. Ed.* 42 (2003) 4068.
- [39] R.R. Davda, J.A. Dumesic, *Chem. Commun.* (2004) 36.